RESPONSE AND VULNERABILITY OF THE ANKLE JOINT IN SIMULATED FOOTWELL INTRUSION EXPERIMENTS – A STUDY WITH CADAVERS AND DUMMIES

Dimitrios Kallieris, Hans Riedl, Rainer Mattern,
Institute of Legal Medicine and Traffic Medicine, University of Heidelberg
Germany
Paper Number: 105

ABSTRACT

The prevention of lower extremity injuries to front seat car occupants is a priority because of their potential to cause long term impairment and disability. To determine the types and mechanisms of lower extremity injuries in frontal collisions, studies under controlled test conditions are needed. Sled tests using belt restrained cadavers and dummies were conducted, in which footwell intrusion was simulated via a plane surface or simulated brake pedal. Human cadavers in the age range from 30 to 62 years and Hybrid III dummies were used.

The footwell intrusion had both translational (135 mm) and rotational (30 degrees) components. Maximum footwell intrusion forces and accelerations were measured. The lower legs were instrumented with accelerometers and a "six axis" force-moment transducer was mounted in the mid shaft of the left tibia. Maximum footwell intrusion forces between 7.4 and 20 kN and accelerations between 31 and 132 g were measured, with the greater values corresponding to the dummy experiments. The maximum axial forces in the tibia amounted to 3.4 – 4.9 kN and the resultant maximum moments were between 61 and 450 Nm. The dummies exhibited significantly higher values than the cadavers.

In the cadaver tests the ankle was dorsiflexed from a neutral position by between 55 and 66 degrees due to the intrusion. The forcing of the ankle joint beyond its normal maximum dorsiflexion angle of approximately 20 degrees results in cartilage contusions, shearing off of the talus and the tibia, fractures of the medial and lateral malleoli, and laceration of the spring ligament. The degree of injury severity depended upon the amount of dorsiflexion and the age. The brake pedal simulation resulted in greater dorsiflexion than the plate intrusion and thereby in a higher injury severity.

INTRODUCTION

While the head and thorax are being protected by a seatbelt and air bag in frontal collisions, a relative increase in foot-ankle injuries in this type of collision has been observed (National Accident Sampling System). The prevention of lower extremity injuries in front seat car occupants has a high priority because of their potential to cause long term impairment and disability. Furthermore these types of injuries have important economic consequences. A calcaneus fracture, for example, is one of the most expensive single injury types (Mattern et al. 1988). To determine the type and mechanisms of lower extremity injuries in frontal collision, studies under controlled test conditions are needed. The study reports on five cadaver and two H III tests.

Test subjects

__Cadavers__ Five cadavers in the age range 30 to 62 years were used in the tests. The most important anthropometric data and the causes of death are listed in Table 1. The research content and the procedures governing the procurement , treatment, and disposal of human surrogates used in this program, conform to the requirements of the Heidelberg University Ethics Commission.

__Dummies__ A 50% male Hybrid III Dummy with ankle rubbers was used (Tests D1, D2)

Table 1.
Anthropometric data

Test No.:	Sex	Age [years]	Weight [kg]	Stature [cm]	Cause of death
C1	male	45	80	179	heart failure
C2	male	30	70	186	acute poisoning
C3	male	62	62	167	head shooting
C4	female	45	75	172	acute poisoning
C5	male	37	79	182	acute poisoning

Test conditions

A frontal impact of 50 km/h was simulated with the sled of the Institute of Legal Medicine and Traffic Medicine of the University of Heidelberg. The sled was decelerated by impacting a metal beam. The sled impact was mechanically coupled to the footwell intrusion device. In tests Nos. 1 to 4 the footwell intrusion was simulated via a plane, in test No. 5 a brake pedal simulator was used. The footwell intrusion had both translational (135 mm) and rotational (30 degrees) components. Furthermore the dashboard and the cabin floor (rigid) were simulated. The cadaver was restrained with a 3 point standard belt. Photographs prior to and after the test are shown in figures 1 and 2. The mean sled deceleration was 15g. Figure 3 shows the sled pulse. The test conditions of test C1 are identical with those of test D1 (without cabin floor). Test C2 is identical with test D2 (with cabin floor), however no tibia force-moment measurements were performed in tests C1 and C2. Tests C3, C4 and C5 are identical with test D2, regarding force-moment measurements in the left tibia.

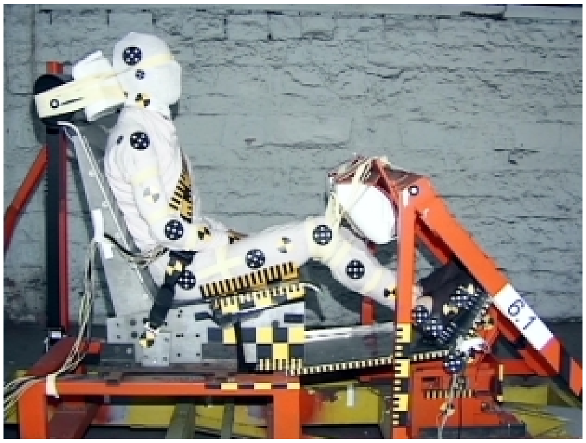

Figure 1.

Lateral view of the belted cadaver prior to test.

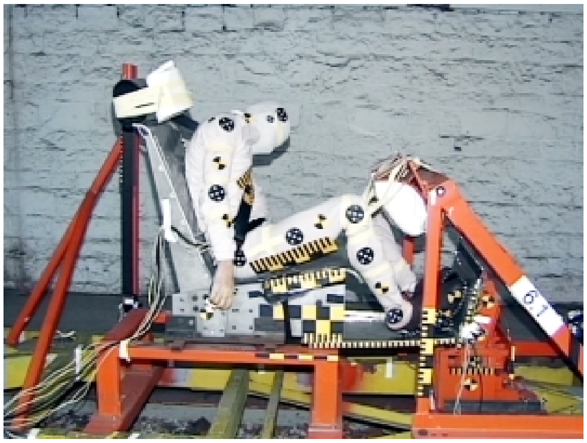

Figure 2.

Lateral view of the belted cadaver after test.

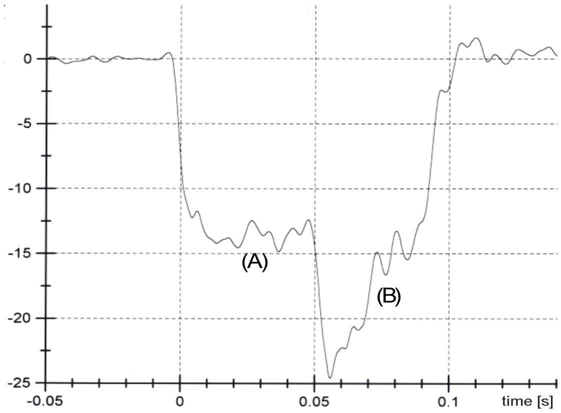

Figure 3.

Sled deceleration-time history
(A): Time interval 0 to 50 ms, part of the original-trapezoidal deceleration time history.
(B): Time interval 50 to 100 ms, deceleration history after activation of the intrusion device.

Instrumentation

Sled and intrusion device

Sled Acceleration:	x-direction
Intrusion Device Acceleration:	x-direction
Footwell Impact Force:	x-direction
Footwell Plate Acceleration:	x- and z-direction upper and lower plate

Cadavers

Pelvis:	Triaxial acceleration at the sacrum
Tibia:	x-, y- and z-acceleration (Tests Nos.: C1, C2 and C5 left and right tibia, Tests Nos.: C3 and C4, right tibia). Semi cylindrical mounts were fixed with wires at the lower third of the tibia. A 3-axial mount was fixed with screws to this semi cylindrical mount.
Left tibia:	In tests C3 to C5 a six axis force-moment transducer (Load cell Model: No.: SP1-5-A (Robert A. Denton)) was connected to the tibia with 2 medullary nails each fixed with 4 screws. Displacement of the nails was prevented by perpendicular mounted pins drilled through the tibia cortical bone. (figures. 4 and 5)

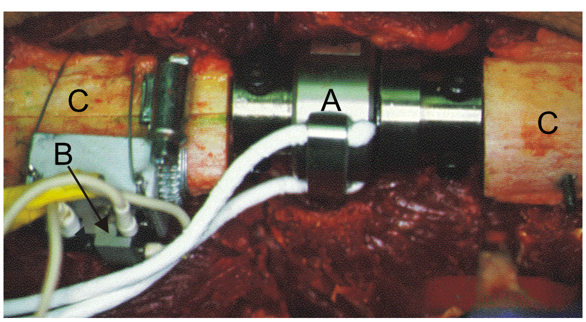

Figure 4.

The force-moment transducer (A) and the fixed 3-axial accelerometer unit (B) at the tibia (C) in situ.

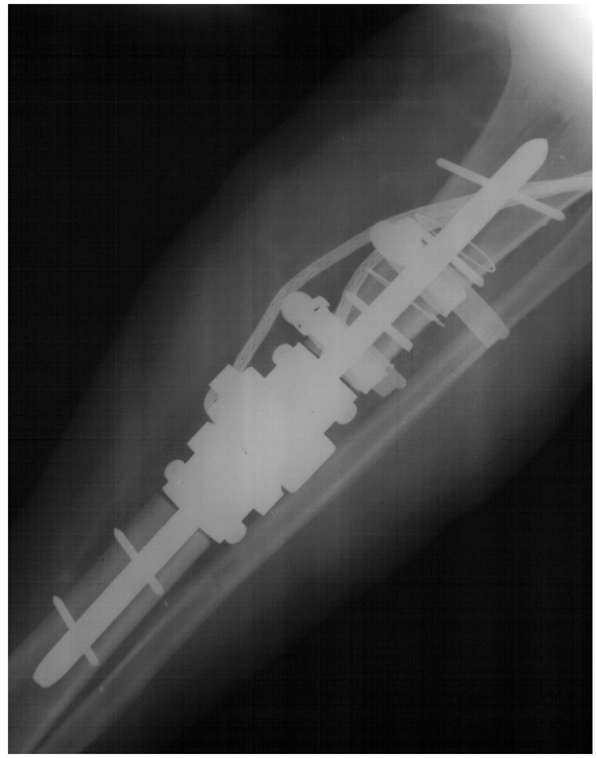

Figure 5.

X-Ray photograph of the force-moment transducer with fixation at the tibia

Dummies

Pelvis:	Acceleration triaxial
Femur:	Force axial left and right
Upper Tibia:	Force axial left and right
Upper Tibia:	Moment M_X left and right
Upper Tibia:	Moment M_Y left and right
Lower Tibia:	Moment M_X left and right
Lower Tibia:	Moment M_Y left and right
Foot:	Acceleration z-direction left and right

Photographic Documentation

Each test was documented with still photographs prior to and after the test. Laterally positioned stationary high speed cine and video cameras both with a frame rate of 1000 Hz captured each test.

Results

Mechanical responses Table 2 summarises the mechanical responses of five cadaver and two Hybrid-III dummy tests. Generally higher values were observed for the Hybrid-III dummy tests than for the cadavers. The greatest differences are present in the tibia moment measurements. The dummy tibia moment was 5 to 7 times higher than that of the cadaver tibia. Fig. 6 shows the tibia force-time histories of cadaver tests C3, C4, C5 and one dummy test D2 performed under identical test conditions and measurement locations. The maximum resultant tibia force is comparable between each cadaver, but was about 40% higher with the Hybrid III dummy.

Table 2.
Maximum and 3ms values for the five cadaver and two dummy tests..

		C1	C2	C3	C4	C5 (**)	D1	D2
Max. footwell force [kN]		7.4	15.8	13.9	18.6	-	>10	20
Max. intrusion acceleration [g]		40	79	43	31	57	132	116
Max. resultant FWP(*) upper [g]		200	304	160	151	170	262	205
Max. resultant FWP lower [g]		120	88	85	85	91	143	89
Res. Acceleration tibia left [g]	max.	247	149	174	132	64	-	-
	3 ms	179	127	133	113	55	-	-
Res. Acceleration tibia right [g]	max.	149	126	120	132	115	-	-
	3 ms	112	107	110	113	110	-	-
Res. force tibia left [kN]	max.	-	-	3.7	3.4	3.6	-	4.9
	3 ms	-	-	3.5	3.2	3.3	-	4.3
Res. moment tibia left [Nm]	max	-	-	90	77	61	-	450
	3 ms	-	-	88	73	58	-	401
Res. Acceleration pelvis [g]	max	18	52	45	40	44	42	44
	3 ms	16	46	42	38	43	-	43
Tibia Index left max.		-	-	0.4	0.4	0.3	-	1.8

(*) FWP: Footwell plate (**) Simulation of brake pedal

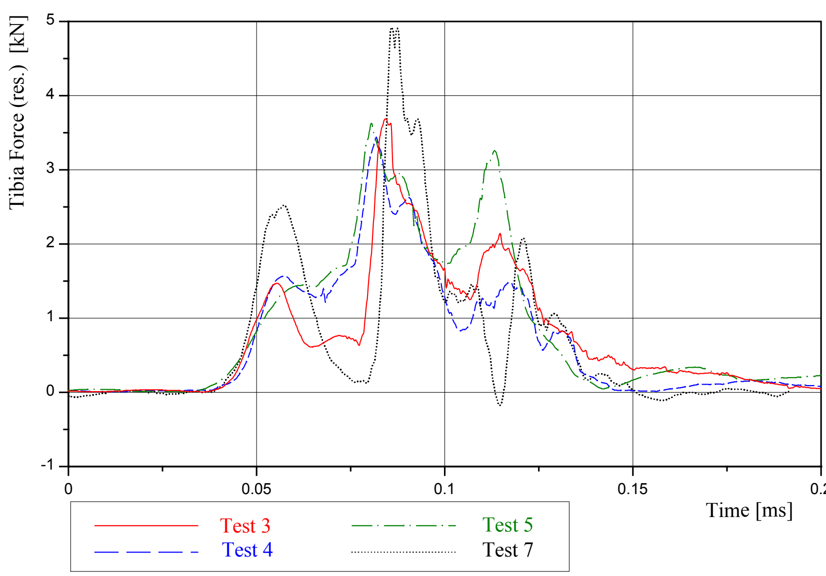

Figure 6.

Resultant tibia force for Tests C3, C4, C5 and D2.

Medical findings

Test C1 Left leg (Fig. 7):
Haemorrhage of the upper ankle joint. The anterior cartilage edge of the joint between the talus and tibia was crushed superficially to a width of 3 cm. 1 x 1 cm sized cartilage haemorrhages at the distal surface of the tibia joint and the upper joint surface of the talus.

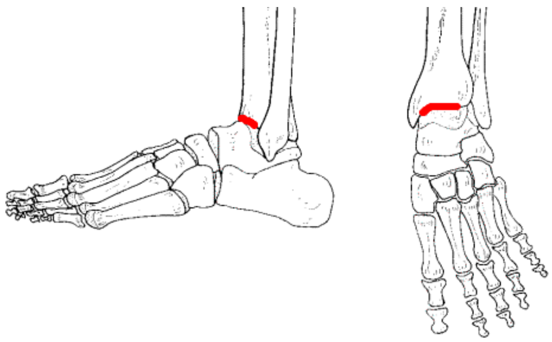

Figure 7.

Injuries of left leg (Test C1)

Test C1 Right leg (Fig. 8):
Transverse fracture of the medial malleolus of the tibia. Cartilage crush at the anterior edge of the inferior joint surface of the tibia across the whole width. About 5mm in diameter sized cartilage contusion at the posterior-lateral talus. Haemorrhages at the talotibial and talonavicular joints. 1 x 1 cm sized cartilage haemorrhages at the distal tibial joint surface and the superior joint surface of the talus.

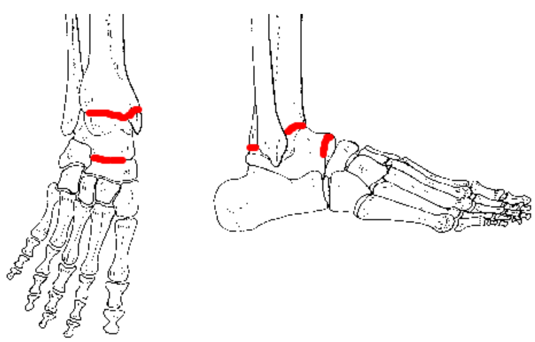

Figure 8.

Injuries of right leg (Test C1)

Test C2 Left leg:
No injuries
Test C2 Right leg:
Central cartilage laceration on the medial side of the patella sized 10mm.
Test C3 Left leg (Fig.9):
Fracture of the medial malleolus. Discrete cartilage shear off of the talus at the talocalcaneal joint.

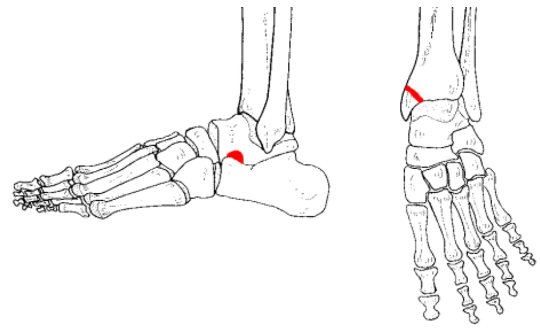

Figure 9.

Injuries of left leg (Test C3)

Test C3: Right leg (Fig.10):
Fracture of the ventral cartilage edge of the tibia with haemorrhage in the joint. Haemorrhage of the ankle joint. Shear off of the cartilage of the plantar side of the talus at the anterior talocalcaneal joint with joint haemorrhage. Edge fracture of the dorso-lateral process of the talus at the talocalcaneal joint in the bony region, medial cartilage laceration caused by compression.

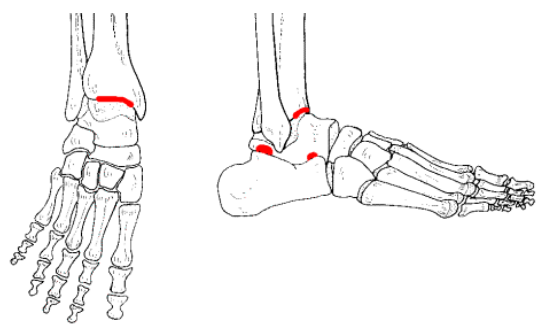

Figure 10.

Injuries of right leg (Test C3)

Test C4: Left leg:
No injuries
Test C4: Right leg :
No injuries
Test C5: Left leg (Figs. 11, 12 and 13):
One horizontally running cartilage contusion sized 2mmx40mm with 2mm deep compression fracture of the anterior tibio-talar joint edge (Figs. 11 and 12). Midline fracture of the lateral malleolus (Fig. 11). Cartilage contusion of the talus with a bruise sized 5mm x 10 mm (Fig.13)

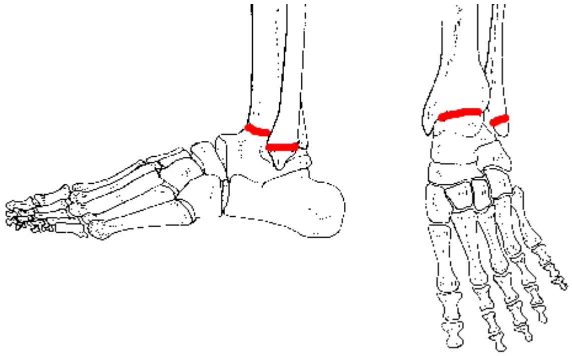

Figure 11.

Injuries of left leg (Test C5)

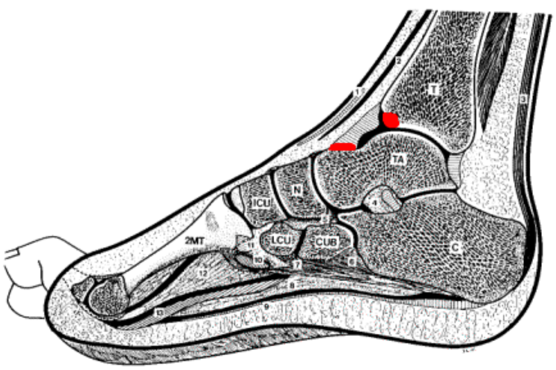

Figure 12.

Injuries of right and left leg (Test C5)

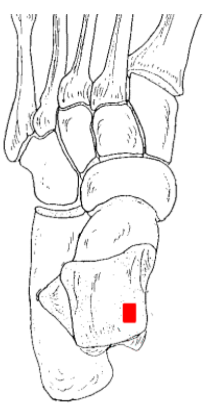

Figure13.

Injury of talus of left leg (Test C5)

<u>Test C5:Right leg</u> (Figs. 12, 14, 15 and 16): Fracture of the medial and lateral malleoli at the level of the tibial joint surface (Fig. 14). Laceration of the spring ligament at the navicular and calcaneal insertion (Fig. 15). Cartilage contusion at the anterior joint surface of the tibia sized 3mm x 40 mm with superficial spongy bone contusion (Figs. 12 and 14). Superficial cartilage shear off of the talus, medial-distal at the near side part of the tibia sized 10mmx10mm (Fig. 16).

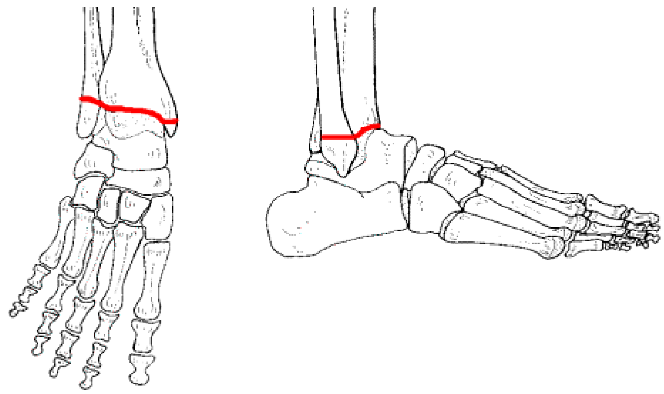

Figure 14.

Injuries of right leg (Test C5)

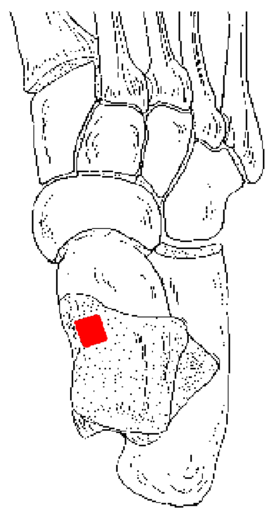

Figure 16.

Injury of talus of right leg (Test C5)

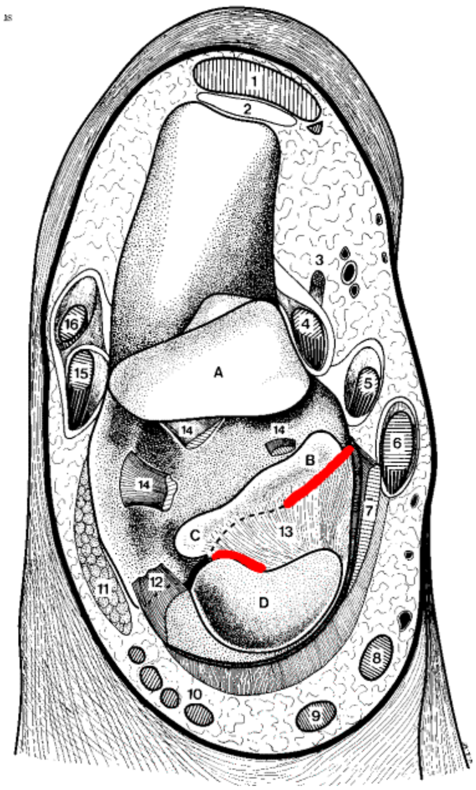

Figure 15.

Talocalcaneal and taleocalcaneonavicular joints (with the talus removed). Superior view.
Laceration of the spring ligament right (Test C5)
(B/C: Middle/anterior articular surface on calcaneus for talus
D: Articular surface on navicular for talus.
13: Spring ligament)

Kinematics of the lower leg and foot.

Due to the construction of the footwell intrusion device the main ankle joint kinematics were forced dorsiflexion. Bending of the lower part of the tibia was also observed. The massive dorsiflexion is reflected in the injury pattern. Figs. 17, 18, 19 and 20 show the variation of the ankle angle during the footwell intrusion for Tests C3, C4, C5 and D2. The variation of the angle between times t=0 ms (φ_0) and t=35 ms (φ_1) and the change in dorsiflexion $\Delta\varphi$ are shown in Table 4. In test C5 the initial angle (φ_0 = 62°) is smaller than in Test C3 and C4 as the break pedal simulator positioned the ankle in more dorsiflexion pre-impact. So for the calculation of the dorsiflexion angle a comparable initial position was identified for C3 and C4 (φ_0 = 84°). Resulting in a maximum change in dorsiflexion angle during test C5 ($\Delta\varphi$. = 65.5°).

Table 4.
Variation of foot-ankle-leg angle during footwell intrusion

Test No.	φ_0 [°] (t=0 ms)	φ_1 [°] (t=35 ms)	$\Delta\varphi$ [°]
C3	83	28	55
C4	84	28.5	55.5
C5	84 (62)	18.5	65.5 (43.5)
D2	87	27	60

Discussion

Five cadaver and two H III dummy tests with simulation of footwell intrusion were performed. The intrusion device was built based on experience with both crash tests and real accident investigation. However sled tests are generally simplified compared to complex road accident situations. Sled tests aim to investigate mechanical responses, injury mechanisms and injury severities. The two Hybrid III dummy tests were conducted to investigate dummy biofidelity. Generally greater lower extremity loads were measured during the dummy tests. In particular the tibia moments were 5 to 7 times greater for the dummy than the cadaver. This can be explained by the higher stiffness of the dummy's "tibia" compared to the human tibia. However the cadaver and dummy showed comparable ankle dorsiflexion.

Two of the five cadavers remained uninjured in the ankle-foot region. This is in accordance with footwell intrusion simulations performed by Crandall (Crandall et al. 1996), who did not observe ankle injuries in every case in sled tests of comparable severity.

In our study the most frequent injury was a malleolar fracture; this type of injuries was also reported by Pieske (Pieske et al. 1998) in real accidents at an impact severity of EES = 25 – 75 km/h. In our tests these injuries were caused by forced dorsiflexion and compression, which was even more extreme, when the break pedal was simulated. As a result of the extreme dorsiflexion fractures of the ventral cartilage edge of the tibia, compression fractures of the anterior tibio-talar joint and shearing-off of the cartilage of the talus were observed. Pieske also reported talus compression fractures due to dorsiflexion caused by high intrusion of the front wall. In our study this severe talus fracture wasn't observed, probably because the amount of dorsiflexion was not great enough. The maximum axial force measured in the tibia was between 3.4 and 3.7 kN. These forces were not sufficient to cause calcaneal fractures in our sample.

<u>Comparison of the lower extremity and ankle kinematics during footwell intrusion.</u>

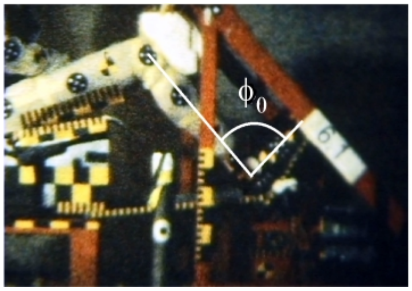

Figure 17a.

Test C3: Start position, t=0 ms, φ_0=83°

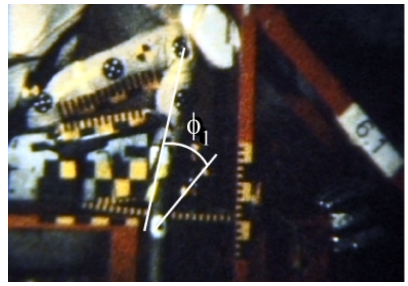

Figure 17b.

Test C3: Maximum dorsiflexion, t=35 ms, φ_1= 28°

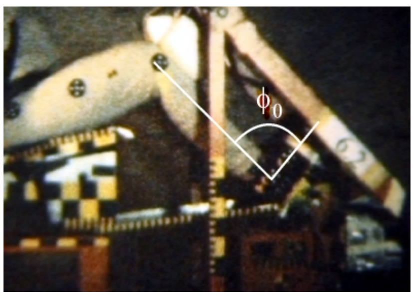

Figure 18a.

Test C4: Start position, t=0 ms, φ_0=84°

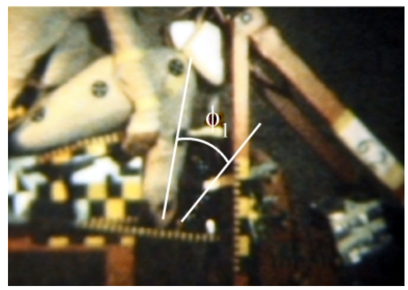

Figure 18b.

Test C3: Maximum dorsiflexion, t=35 ms, φ_1= 28.5°

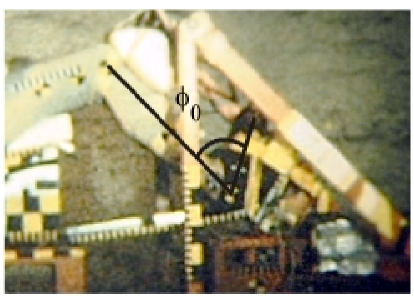

Figure 19a.

Test C5: Start position, t=0 ms, φ_0=62°

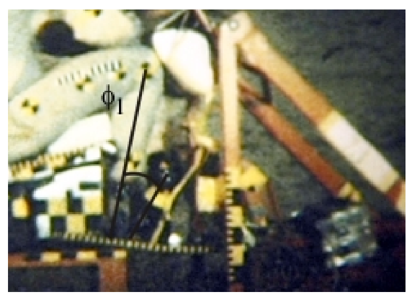

Figure 19b.

Test C5: Maximum dorsiflexion, t=35 ms, φ_1= 18.5°

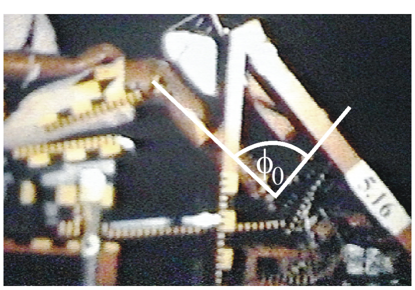

Figure 20a.

Test D2: Start position, t=0 ms, φ_0=87°

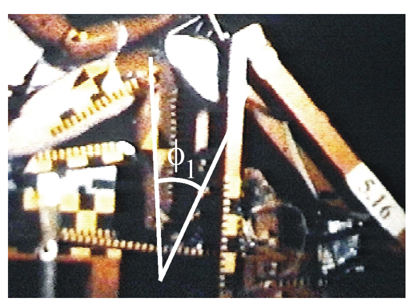

Figure 20b.

Test D2: Maximum dorsiflexion, t=35 ms, φ_1= 27°

Crandall et al. also observed these fractures in sled experiments with an axial tibia force of only 1 kN, while McMaster (McMaster et al. 2000) and Kitagawa (Kitagawa et al. 1998) observed calcaneal fractures at axial tibia loads from 3.8 to 9 kN in impactor tests with isolated legs. In the latter tests the legs were fixed at the knee region and were restrained from turning aside. This situation isn't comparable to real accidents and can only be used for the investigation of the biomechanical properties of the foot-ankle-leg complex. According to our biomechanical experience the fracture level is age dependent. Although calcaneal fractures were not found in our study, calcaneus and talus fractures are the most frequent observed fracture types (37%) in real accident cases (Pieske et al. 1998). We also consider the reaction of the driver or front passenger, e.g. pressing of the feet against the front wall, as another factor, which can explain this discrepancy. To conclude, it is not possible to compare directly injuries from road accidents to crash tests performed with cadavers without considering the severity of the real individual accident.

Literature

Crandall JR, Bass CR, Klopp GS, Pilkey WD (1996) Sled Test Toepan Intrusion Using Post-mortem Human Surrogates and the Hybrid-III-Dummy. Proc. of the Ircobi Conference, p 339-352

Kitagawa Y, Ichikawa H, King AI and Levine RS, (1998) A Severe Ankle and Foot Injury in Frontal Crashes and Its Mechanism, SAE Paper No.: 983145 Proc. of the 42nd Stapp Car Crash Conf., p 1-12

Mattern R et al. (1988) Verletzungskosten nach Straßenverkehrsunfällen, FAT-Schriftenreihe Nr. 73

National Accident Sampling System: Weighted Distribution of Injuries by Body Region for Unbelted Occupants, Belted Occupants and for Drivers in Cars with air bag Deployment During the Accident (AIS 2+, 1990 – 1992)

McMaster J, Parry M, Wallace W A, Wheeler L, Owen C, Lowne R, Oakley C, Roberts AK (2000) Biomechanics of Ankle and Hindfoot Injuries in Dynamic Axial Loading, Stapp Car Crash Journal 44, , p 357-377

Pieske O, Lob G, Nüzel S; Messner G and Schönpflug M (1998) Die Belastung der unteren Extremität bei Autounfällen, Hefte zu "Der Unfallchirurg", Springer, p 60-64

Acknowledgements

The authors wish to gratefully acknowledge the European Community for the support of ADRIA Project No.: PL96-1074 and FID Project No.: GRD1-1990-10559. We also thank Robert Denton Inc. for the donation of the force and moment transducer.